JVI Journals.ASM.org

Human Coronavirus NL63 Utilizes Heparan Sulfate Proteoglycans for Attachment to Target Cells

Aleksandra Milewska,[a] Miroslaw Zarebski,[b] Paulina Nowak,[a] Karol Stozek,[a] Jan Potempa,[a,c] Krzysztof Pyrc[a,d]

Microbiology Department, Faculty of Biochemistry, Biophysics and Biotechnology, Jagiellonian University, Krakow, Poland[a]; Division of Cell Biophysics, Faculty of Biochemistry, Biophysics and Biotechnology, Jagiellonian University, Krakow, Poland[b]; Department of Oral Immunology and Infectious Diseases, School of Dentistry, University of Louisville, Louisville, Kentucky, USA[c]; Laboratory of Virology, Malopolska Centre of Biotechnology, Jagiellonian University, Krakow, Poland[d]

ABSTRACT

Human coronavirus NL63 (HCoV-NL63) is an alphacoronavirus that was first identified in 2004 in the nasopharyngeal aspirate from a 7-month-old patient with a respiratory tract infection. Previous studies showed that HCoV-NL63 and the genetically distant severe acute respiratory syndrome (SARS)-CoV employ the same receptor for host cell entry, angiotensin-converting enzyme 2 (ACE2), but it is largely unclear whether ACE2 interactions are sufficient to allow HCoV-NL63 binding to cells. The present study showed that directed expression of angiotensin-converting enzyme 2 (ACE2) on cells previously resistant to HCoV-NL63 renders them susceptible, showing that ACE2 protein acts as a functional receptor and that its expression is required for infection. However, comparative analysis showed that directed expression or selective scission of the ACE2 protein had no measurable effect on virus adhesion. In contrast, binding of HCoV-NL63 to heparan sulfates was required for viral attachment and infection of target cells, showing that these molecules serve as attachment receptors for HCoV-NL63.

IMPORTANCE

ACE2 protein was proposed as a receptor for HCoV-NL63 already in 2005, but an in-depth analysis of early events during virus infection had not been performed thus far. Here, we show that the ACE2 protein is required for viral entry but that it is not the primary binding site on the cell surface. Conducted research showed that heparan sulfate proteoglycans function as adhesion molecules, increasing the virus density on cell surface and possibly facilitating the interaction between HCoV-NL63 and its receptor. Obtained results show that the initial events during HCoV-NL63 infection are more complex than anticipated and that a newly described interaction may be essential for understanding the infection process and, possibly, also assist in drug design.

Coronaviruses (CoVs) are enveloped positive-stranded RNA viruses with large genomes ranging in size from 27 to 32 kb. Six human coronaviruses (HCoVs) have been identified to date, and four of them (HCoV-229E, HCoV-OC43, HCoV-NL63, and HCoV-HKU1) are thought to be responsible for ~30% of common cold cases (1). In contrast, infection with severe acute respiratory syndrome coronavirus (SARS-CoV) results in a serious respiratory tract infection, which in the 2002-2003 season affected approximately 8,000 patients, with a mortality rate of ~10% (2, 3). Similarly, the recently isolated Middle East respiratory syndrome coronavirus (MERS-CoV) causes life-threatening pneumonia and renal failure, with almost 300 fatal cases reported to date (4).

Human coronavirus NL63 was first identified in 2004 in the nasopharyngeal aspirate from a 7-month-old patient with a respiratory tract infection. The virus is distributed worldwide and causes respiratory infections of varying severity, with the most severe symptoms seen in children and immunocompromised patients (5–9).

Like other human coronaviruses, the HCoV-NL63 genome encodes a glycoprotein, called the spike (S) protein, which protrudes from the virion surface, thereby conferring the corona-like form (6, 10, 11). The S protein is the main mediator of viral entry and determines the host tropism of the coronavirus (12, 13). A study undertaken in 2005 used retroviral reporter pseudoviruses carrying the HCoV-NL63 spike (NL63-S) protein to show that HCoV-NL63 engages the SARS-CoV receptor, angiotensin-converting enzyme 2 (ACE2), for infectious entry (14–16). ACE2 is a type I integral membrane protein abundantly expressed in tissues lining the respiratory tract. This carboxypeptidase cleaves angiotensin II and functions within the renin-angiotensin system (RAS) important for maintaining lung homeostasis and blood pressure (17–19). Downregulation of ACE2 protein levels may lead to the development of acute respiratory distress syndrome. Thus, downregulation of ACE2 expression in the lungs upon SARS-CoV infection is associated with viral pathogenesis (20–23).

HCoV-NL63 can be cultured in monkey epithelial cell lines that endogenously express ACE2 (e.g., LLC-Mk2, Vero E6, or Vero B4 cells), as well as in the human hepatoma cell line, Huh-7; this host preference is shared with SARS-CoV (24–26). Hofmann et al. (14) conducted a thorough analysis of the cellular tropism of these two human coronaviruses and found out that pseudovirions bearing the spike proteins of HCoV-NL63 (NL63-S) and SARS-CoV (SARS-S) showed similar abilities to infect target cells. However, some studies show that the SARS-CoV S protein has a higher affinity for ACE2 than the HCoV-NL63 S protein (20, 27).

Even though the cellular receptor for HCoV-NL63 was described previously, until the present it was unknown whether ACE2 serves as an adhesion factor and is sufficient to facilitate viral entry. Here, we show that directed expression of the ACE2

Received 16 July 2014 **Accepted** 27 August 2014
Published ahead of print 3 September 2014
Editor: S. Perlman
Address correspondence to Krzysztof Pyrc, k.a.pyrc@uj.edu.pl.

doi:10.1128/JVI.02078-14

protein renders the cells permissive to HCoV-NL63 infection. Interestingly, the presence of the receptor protein does not seem to correlate with the adhesion of virions to cell surface, hence suggesting the presence of yet another factor important during early stages of infection. Subsequent analysis showed that heparan sulfate (HS) proteoglycans function as adhesion receptors for HCoV-NL63, complementing the action of the ACE2 protein. Assessment of viral replication dynamics clearly shows that the adhesion of HCoV-NL63 to heparin sulfate proteoglycans enhances viral infection.

MATERIALS AND METHODS

Cell culture. LLC-Mk2 cells (ATCC CCL-7; *Macaca mulatta* kidney epithelial cells) were maintained in minimal essential medium (MEM; two parts Hanks' MEM and one part Earle's MEM [Life Technologies, Poland]) supplemented with 3% heat-inactivated fetal bovine serum (Life Technologies, Poland), penicillin (100 U ml^{-1}), streptomycin (100 μg ml^{-1}), and ciprofloxacin (5 μg ml^{-1}). Human 293T (ATCC CRL-3216; kidney epithelial cells) and A549 (ATCC CCL-185; lung carcinoma cells) cells were maintained in Dulbecco's MEM (Life Technologies, Poland) supplemented with 10% heat-inactivated fetal bovine serum (Life Technologies, Poland), penicillin (100 U ml^{-1}), streptomycin (100 μg ml^{-1}), and ciprofloxacin (5 μg ml^{-1}). Cells were cultured at 37°C under 5% CO_2.

Isolation of nucleic acids and reverse transcription. HCoV-NL63 nucleic acids were isolated from cell culture supernatants using a Total RNA Mini-Preps Super kit (Bio Basic, Canada), according to the manufacturer's instructions. Reverse transcription was carried out with a high-capacity cDNA reverse transcription kit (Life Technologies, Poland), according to the manufacturer's instructions.

Cell lines expressing ACE2. 293T cells (ATCC CRL-3216) were transfected with the pLKO.1-TRC-ACE2 plasmid using polyethylenimine (PEI; Sigma-Aldrich, Poland). The plasmid was based on the Addgene plasmid 10878 (28). At 24 h posttransfection, the cells were washed with sterile 1× phosphate-buffered saline (PBS) and cultured at 37°C for 48 h in medium supplemented with puromycin (2 μg ml^{-1}) at 37°C with 5% CO_2. Following selection, cells were passaged, and the surviving clones were collected and analyzed as described below. ACE2-expressing ($ACE2^+$) cells were maintained in Dulbecco's MEM supplemented with 10% heat-inactivated fetal bovine serum, penicillin (100 U ml^{-1}), streptomycin (100 μg ml^{-1}), ciprofloxacin (5 μg ml^{-1}), and puromycin (1 μg ml^{-1}).

ACE2-expressing A549 cells (A549_$ACE2^+$) were generated using retroviral vectors that were based on a Moloney murine leukemia virus system. Briefly, Phoenix-AMPHO cells (ATCC CRL-3213) were transfected with a pLNCX2 vector (Clontech, USA) encoding the ACE2 protein using PEI. At 24 h posttransfection, the medium was refreshed, and the cells were cultured for a further 24 h at 32°C. Subsequently, the vector-containing supernatants were harvested, aliquoted, and stored at −80°C.

Wild-type (WT) A549 cells (A549_WT) cells were cultured in six-well plates (TPP, Switzerland) and infected with 1 ml of generated retroviruses in the presence of Polybrene (5 μg ml^{-1}; Sigma-Aldrich). After 24 h of incubation at 37°C, the cells were cultured in medium supplemented with G418 (5 mg ml^{-1}; BioShop, Canada) and passaged for 3 weeks at 37°C. Surviving clones were recovered and analyzed as described below. A549_$ACE2^+$ cells were maintained in Dulbecco's MEM supplemented with 10% heat-inactivated fetal bovine serum, penicillin (100 U ml^{-1}), streptomycin (100 μg ml^{-1}), ciprofloxacin (5 μg ml^{-1}), and G418 (5 mg ml^{-1}).

Virus preparation, titration, and cell infection. The HCoV-NL63 stock (isolate Amsterdam 1) was generated by infecting monolayers of LLC-Mk2 cells. Cells were then lysed by two freeze-thaw cycles at 6 days postinfection (p.i.). The virus-containing liquid was aliquoted and stored at −80°C. A control LLC-Mk2 cell lysate from mock-infected cells was prepared in the same manner. The virus yield was assessed by titration on fully confluent LLC-Mk2 cells in 96-well plates, according to the method of Reed and Muench (29). Plates were incubated at 32°C for 6 days, and the cytopathic effect (CPE) was scored by observation under an inverted microscope.

In subsequent experiments, fully confluent cells (WT 293T cells or 293T cells expressing ACE2 [293T_WT/$ACE2^+$] and A549_WT/$ACE2^+$) in six-well plates (TPP) were exposed to HCoV-NL63 at a 50% tissue culture infective dose ($TCID_{50}$) ml^{-1} of 5,000. HCoV-NL63-permissive LLC-Mk2 cells were infected with the virus at a $TCID_{50}$ ml^{-1} of 400. Following a 2-h incubation at 32°C, unbound viruses were removed by washing with sterile 1× PBS, and fresh medium was added to each well. Samples of cell culture supernatant were collected every 24 h for 6 days and analyzed by real-time PCR.

Quantitative PCR. The virus yield was determined using real-time PCR (7500 Fast Real-Time PCR machine; Life Technologies, Poland). Viral cDNA (2.5 μl per sample) was amplified in a 10-μl reaction mixture containing 1× TaqMan Universal PCR master mix (Life Technologies, Poland), specific probes labeled with 6-carboxyfluorescein (FAM) and 6-carboxytetramethylrhodamine (TAMRA) (100 nM), and primers (450 nM each). The following primers were used for HCoV-NL63 amplification: sense, 5′-AAA CCT CGT TGG AAG CGT GT-3′; antisense, 5′-CTG TGG AAA ACC TTT GGC ATC-3′; probe, 5′-FAM-ATG TTA TTC AGT GCT TTG GTC CTC GTG AT-TAMRA-3′. ROX (6-carboxy-X-rhodamine) was used as the reference dye. The reaction conditions were as follows: 2 min at 50°C and 10 min at 92°C, followed by 40 cycles of 15 s at 92°C and 1 min at 60°C.

Gradient purification of HCoV-NL63. The virus stock was concentrated 25-fold using centrifugal protein concentrators (Amicon Ultra, 10-kDa cutoff; Merck, Poland) and subsequently layered onto a 15% iodixanol solution in 1× PBS (OptiPrep medium; Sigma-Aldrich, Poland). Following centrifugation at 175,000 × *g* for 3 h at 4°C (cushion), virus-containing fractions were layered onto a 10 to 20% iodixanol gradient (in 1× PBS) and centrifuged at 175,000 × *g* for 18 h at 4°C. Fractions collected from the gradient were analyzed by Western blotting, followed by detection of the HCoV-NL63 nucleocapsid (NL63-N) protein. The resulting virus-containing fractions were aliquoted and stored at −80°C. The control cell lysate (mock) was prepared in the same manner as the virus stock.

Detection of sgmRNAs. Total nucleic acids were isolated from virus- and mock-infected cells at 5 days p.i. using a Total RNA Mini-Preps Super kit (Bio Basic, Canada), according to the manufacturer's instructions. Reverse transcription was performed using a high-capacity cDNA reverse transcription kit (Life Technologies, Poland), according to the manufacturer's instructions. Viral cDNA (3 μl) was amplified in a 20-μl reaction mixture containing 1× Dream *Taq* Green PCR master mix and primers (each primer was used at 500 nM). The following primers were used to amplify HCoV-NL63 subgenomic mRNA (sgmRNA): common sense primer (leader sequence), 5′-TAA AGA ATT TTT CTA TCT ATA GAT AG-3′; 1a/b polyprotein antisense, 5′-CAT CAA AGT CCT GAA GAA CAT AAT TG-3′; spike antisense, 5′-ACT ACG GTG ATT ACC AAC ATC AAT ATA-3′; spike (nested PCR) antisense, 5′-AGA GAT TAG CAT TAC TAT TAC ATG TG-3′; open reading frame 3 (ORF3) antisense, 5′-GCA CAT AGA CAA ATA GTG TCA ATA GT-3′; envelope (E) antisense, 5′-GCT ATT TGC ATA TAA TCT TGG TAA GC-3′; membrane (M) antisense, 5′-GAC CCA GTC CAC ATT AAA ATT GAC A-3′; nucleocapsid antisense, 5′-CTT ATG AGG TCC AGT ACC TAG GTA AT-3′. The conditions were as follows: 3 min at 95°C, 40 cycles (30 cycles for nested PCR) of 30 s at 95°C, 30 s at 47°C, and 25 s at 72°C, followed by 5 min at 72°C and 10 min at 4°C. The PCR products were run on 1% agarose gels (1× Tris-acetate EDTA [TAE] buffer) and analyzed using molecular imaging software (Kodak).

Western blot analysis. Cells used for Western blot analysis were harvested at 5 days p.i. by scraping in ice-cold 1× PBS. The cells were then centrifuged and resuspended in radioimmunoprecipitation assay (RIPA) buffer (50 mM Tris, 150 mM NaCl, 1% Nonidet P-40, 0.5% sodium deoxycholate, 0.1% SDS, pH 7.5), followed by lysis in RIPA buffer for 30 min on ice. Subsequently, samples were centrifuged (10 min at 12,000 × *g*), and the pelleted cell debris was discarded. Total protein concentration of

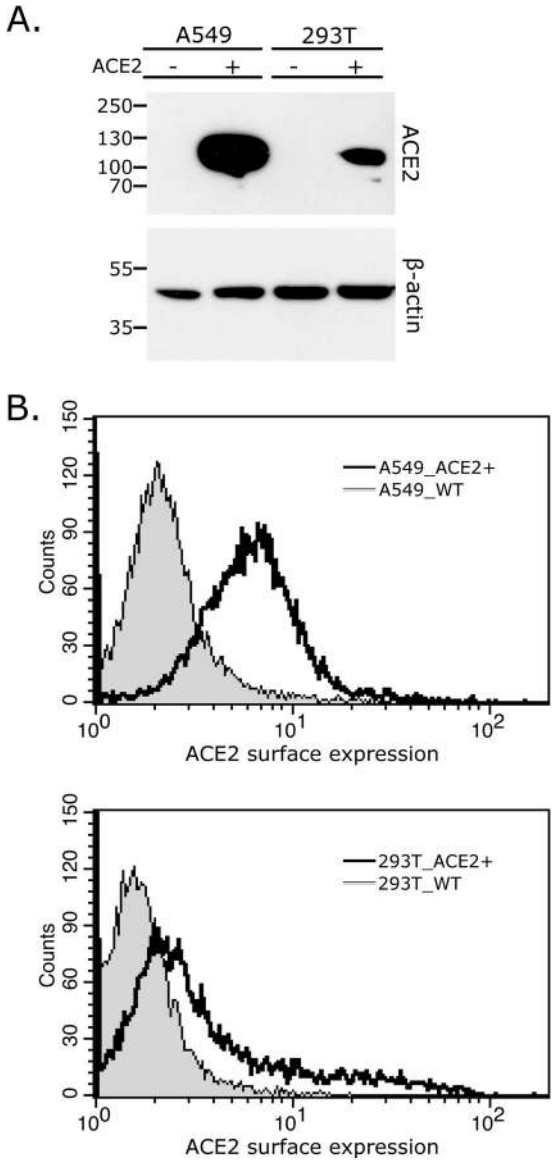

FIG 1 Human cell lines overexpressing ACE2 protein. (A) Lysates of A549_ACE2$^+$ (A549 +) and A549_WT (A549 −) cells and of 293T_ACE2$^+$ (293T +) and 293T_WT (293T −) cells were tested for the presence of the ACE2 protein with Western blotting using antibodies specific to the ectodomain of the human ACE2 protein. Concomitantly, β-actin protein levels were assessed in each sample. Numbers on the left side represent molecular mass (kDa) assessed with a size marker. The results shown are representative of at least three independent experiments. (B) A549_ACE2$^+$, A549_WT, 293T_ACE2$^+$, and 293T_WT cells were tested for the surface expression of the ACE2 protein with flow cytometry using antibodies specific to the ectodomain of the human ACE2 protein. The results shown are representative of at least three independent experiments.

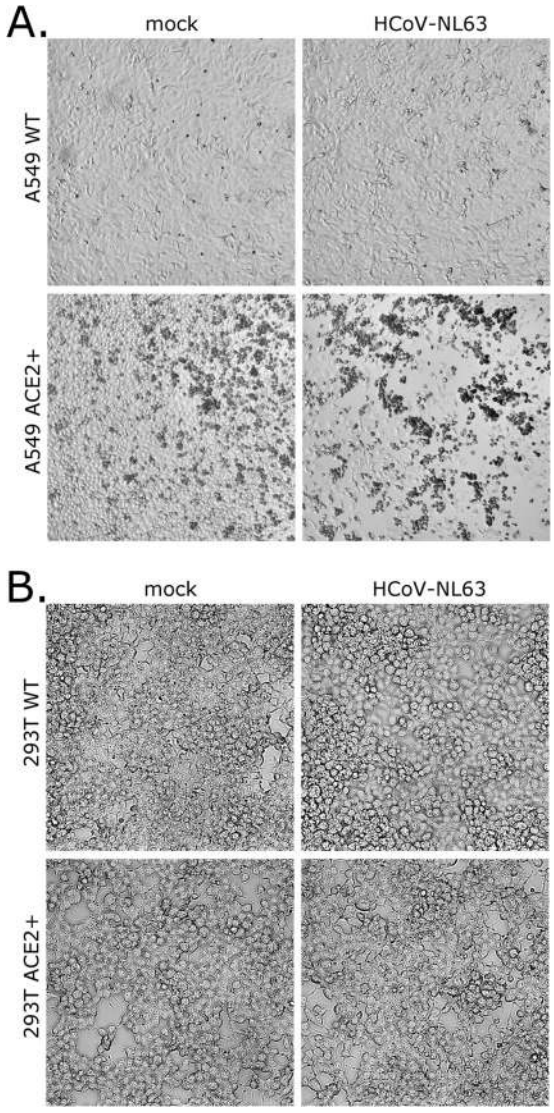

FIG 2 Cytopathic effect on A549_ACE2$^+$ cells during HCoV-NL63 infection. ACE2-overexpressing (ACE2$^+$) and wild-type (WT) A549 and 293T cells were infected with HCoV-NL63 or mock inoculated and cultured for 6 days. Cytopathic effect was observed only on HCoV-NL63-infected A549_ACE2$^+$ cells. Magnification, ×200. The results shown are representative of at least three independent experiments.

each sample was quantified using the bicinchoninic acid (BCA) method, and the resulting supernatants were mixed with sample buffer (0.5 M Tris, pH 6.8, 10% SDS, 50 mg/ml dithiothreitol [DTT]), boiled for 5 min, cooled on ice, and separated on 10% polyacrylamide gels alongside dual-color PageRuler prestained protein size markers (Thermo Scientific, Poland). The separated proteins were then transferred onto a Westran S polyvinylidene difluoride (PVDF) membrane (Whatman) by semidry blotting (Bio-Rad) for 1.5 h at 100 V in transfer buffer consisting of 25 mM Tris, 192 mM glycine, and 20% methanol at 4°C. The membranes were then blocked by overnight incubation (at 4°C) in Tris-buffered saline (TBS)-Tween (0.1%) buffer supplemented with 5% skimmed milk (Bio-Shop, Canada). A goat anti-human ACE2 ectodomain antibody (2 μg ml^{-1}; R&D Systems, USA) and horseradish peroxidase (HRP)-labeled rabbit anti-goat IgG (26 ng ml^{-1}; Dako, Denmark) were used to detect the ACE2 protein in human cell lysates and cell supernatants. A mouse anti-HCoV-NL63-N protein antibody (500 ng ml^{-1}; Ingenansa, Spain) and horseradish peroxidase-labeled rabbit anti-mouse IgG (65 ng ml^{-1}; Dako, Denmark) were used to detect the HCoV-NL63 nucleocapsid protein. A mouse anti-β-actin antibody (50 ng ml^{-1}; BD Biosciences, USA) and horseradish peroxidase-labeled rabbit anti-mouse IgG (65 ng ml^{-1}; Dako, Denmark) were used for detection of β-actin. All antibodies were diluted in 1% skimmed milk plus TBS-Tween (0.1%). The signal was developed using an Immobilon Western Chemiluminescent HRP Substrate (Millipore) and visualized by exposing the membrane to an X-ray film (Kodak).

Flow cytometry. A549 WT and ACE2$^+$ cells and LLC-Mk2 cells were seeded in six-well plates (TPP, Switzerland), cultured for 2 days at 37°C,

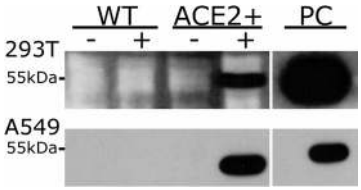

FIG 3 HCoV-NL63 nucleocapsid protein expression in ACE2$^+$ cells. ACE2$^+$ and WT 293T and A549 cells were infected with HCoV-NL63 (+) or mock infected (−). HCoV-NL63 nucleocapsid protein was detected at 6 days p.i. in A549_ACE2$^+$ and 293T_ACE2$^+$ cell lysates, suggesting viral replication. No signal from the NL63-N protein was observed in mock-infected cells. A sample containing lysate of LLC-Mk2 cells infected with HCoV-NL63 was used as a positive control (PC). The position of the 55-kDa molecular mass marker is shown on the left side. The results shown are representative of at least three independent experiments.

and stimulated with phorbol 12-myristate 13-acetate ([PMA] 1 μM; Sigma-Aldrich, Poland) for 1 h at 37°C. To examine HCoV-NL63 adhesion, cells were washed with 1× PBS and incubated with iodixanol-concentrated HCoV-NL63 or a mock control for 2 h at 4°C. The cells were then washed with 1× PBS, fixed with 3% paraformaldehyde (PFA), permeabilized with 0.1% Triton X-100 in 1× PBS, and incubated for 1 h with 3% bovine serum albumin (BSA)–0.1% Tween 20 in 1× PBS. To examine the HCoV-NL63 adhesion, cells were mechanically detached from the plate surface and incubated for 2 h at room temperature with a mouse anti-HCoV-NL63-N antibody (1 μg ml^{-1}; Ingenansa, Spain), followed by 1 h of incubation with an Alexa Fluor 488-labeled goat anti-mouse antibody (2.5 μg ml^{-1}; Molecular Probes). For ACE2 staining, cells were washed with 1× PBS, scraped from the plates, and incubated for 2 h at 4°C with goat anti-ACE2 ectodomain IgG (4 μg ml^{-1}; R&D Systems, USA), followed by 1 h of incubation with a fluorescein isothiocyanate (FITC)-

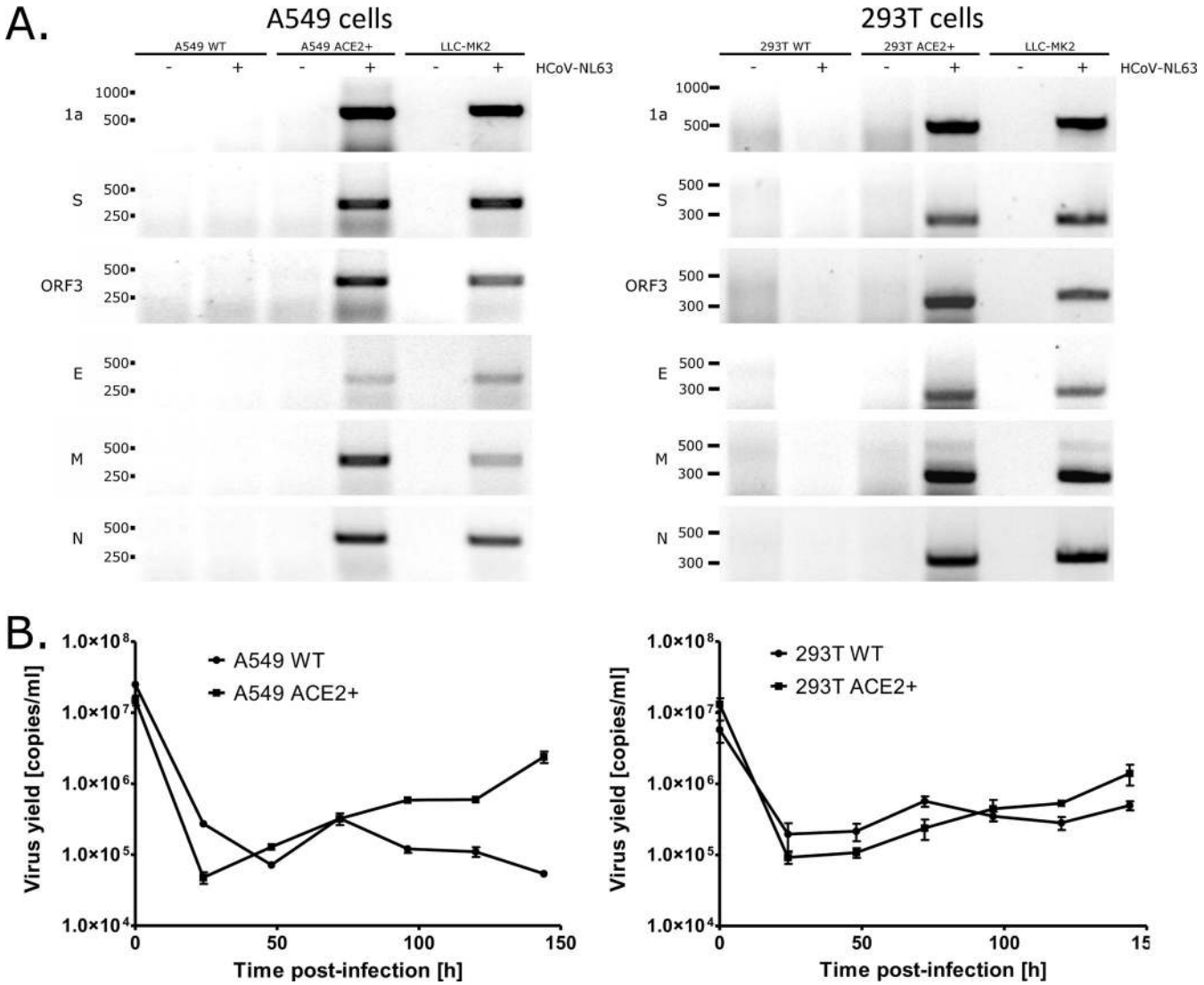

FIG 4 HCoV-NL63 replication in ACE2-overexpressing cells. ACE2-overexpressing and wild-type cells were infected with HCoV-NL63 (+) or mock infected (−) and cultured for 6 days. (A) Genomic RNA (1a) and a set of HCoV-NL63 sgmRNAs, including spike (S), ORF3, envelope (E), membrane (M), and nucleocapsid (N), were detected in A549_ACE2$^+$ and 293T_ACE2$^+$ cells. No HCoV-NL63 sgmRNAs were detected in WT cells. LLC-Mk2 cells infected with HCoV-NL63 (+) or mock infected (−) were used as controls. Positions of nucleotide size markers are shown on the left side of each panel. The results shown are representative of at least three independent experiments. (B) HCoV-NL63 replication on A549 and 293T cells was evaluated with real-time PCR. A marked increase in virus yield was observed on A549_ACE2$^+$ cells and, to a much lesser extent, on 293T_ACE2$^+$ cells. No increase in virus yield was observed on HCoV-NL63-infected A549 and 293T WT cells. Data on virus replication are presented as the number of HCoV-NL63 RNA copies/ml. All assays were performed in triplicate, and average values with standard errors (error bars) are presented.

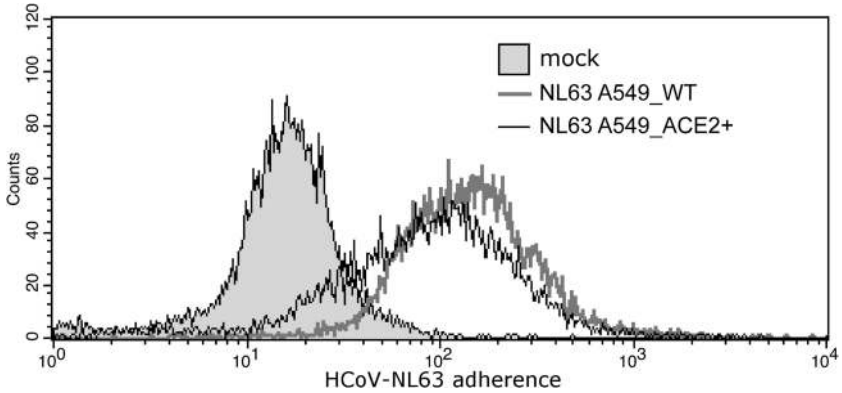

FIG 5 Directed expression of the ACE2 protein on A549 cells does not alter HCoV-NL63 adhesion. Analysis of HCoV-NL63 adherence to ACE2-overexpressing ($ACE2^+$) or wild-type (WT) A549 cells was conducted with flow cytometry. The results shown are representative of at least three independent experiments.

labeled rabbit anti-goat IgG antibody (13 μg ml^{-1}; Dako, Denmark). Cells were then washed, resuspended in 1× PBS, and analyzed by flow cytometry (FACSCalibur; Becton Dickinson). Data were analyzed using Cell Quest software (Becton Dickinson).

Confocal microscopy. LLC-Mk2 cells were seeded on coverslips in six-well plates (TPP), cultured for 2 days at 37°C, and then stimulated with PMA (1 μM; Sigma-Aldrich, Poland) for 1 h at 37°C. Subsequently, the cells were washed with 1× PBS and incubated with iodixanol-concentrated HCoV-NL63 or a mock control for 2 h at 4°C. Cells were then washed with 1× PBS, fixed with 3% PFA, permeabilized with 0.1% Triton X-100 in 1× PBS, and incubated for 1 h with 5% BSA–0.5% Tween 20 in 1× PBS. To visualize HCoV-NL63 adhesion, cells were incubated for 2 h at room temperature with mouse anti-NL63-N IgG (0.25 μg ml^{-1}; Ingenansa, Spain), followed by 1 h of incubation with Alexa Fluor 488-labeled goat anti-mouse IgG (2.5 μg ml^{-1}; Life Technologies, Poland). Nuclear DNA staining was performed with 4′,6′-diamidino-2-phenylindole ([DAPI] 0.1 μg ml^{-1}; Sigma-Aldrich, Poland). Immunostained cultures were mounted on glass slides in Vectashield medium (Vector Laboratories, United Kingdom). Fluorescent images were acquired under a Leica TCS SP5 II confocal microscope (Leica Microsystems GmbH, Mannheim, Germany). Images were acquired using Leica Application Suite Advanced Fluorescence (LAS AF) software, version 2.2.1 (Leica Microsystems CMS GmbH), deconvolved with Huygens Essential package, version 4.4 (Scientific Volume Imaging B.V., The Netherlands), and processed using ImageJ, version 1.47 (National Institutes of Health, Bethesda, MD, USA). Viruses attached to the cell were quantified using a three-dimensional (3D) object counter plug-in for ImageJ (30) with the histogram threshold set to 80. Analysis was performed on *z*-stacks (step size, 0.13 μm) of at least 10 cells per sample.

Assessing the effects of neuraminidase on virus adherence. LLC-Mk2 cells were seeded in six-well plates (TPP, Switzerland), cultured for 2 days at 37°C, and incubated with type V neuraminidase (from *Clostridium perfringens*; 100 to 200 mU/ml [Sigma-Aldrich, Poland]) for 1 h at 37°C. The adherence of iodixanol-concentrated HCoV-NL63 was examined as described above.

Assessing the effects of sugars and heparan sulfate on virus replication and adherence. LLC-Mk2 cells were seeded in six-well plates (TPP, Switzerland), cultured for 2 days at 37°C, and incubated with sugar monomers (50 mM; Sigma-Aldrich, Poland) or heparan sulfate (HS; Sigma-Aldrich, Poland) for 1 h at 37°C. Simultaneously, iodixanol-concentrated HCoV-NL63 was incubated with tested compounds for 1 h at 4°C, and virus adherence was examined as described above. To assess HCoV-NL63 replication, cells were washed with 1× PBS and infected with virus preincubated with HS at a $TCID_{50}$ ml^{-1} of 100. Following 2 h of incubation at 32°C, unbound virus was removed by washing with 1× PBS, and fresh medium containing HS was added to each well. Samples of cell culture supernatant were collected at 6 days postinfection and analyzed in a real-time PCR assay.

RESULTS

Development of cell lines expressing the ACE2 protein. Human cell lines stably expressing the ACE2 receptor (A549 and 293T) were developed in-house. Expression and surface localization of the ACE2 protein were confirmed by Western blotting (Fig. 1A) and flow cytometry (Fig. 1B), respectively.

ACE2 acts as a receptor for HCoV-NL63 and is sufficient to enable infectious entry. Human cell lines expressing the ACE2 protein were used to determine whether surface expression of ACE2 is sufficient for HCoV-NL63 entry. Both $ACE2^+$ and WT A549 and 293T cells were infected with HCoV-NL63 and cultured for 6 days at 32°C. Infection of A549_$ACE2^+$ cells resulted in clear CPE at 3 days p.i.; no CPE was observed in HCoV-NL63-infected A549_WT cells and 293T_WT/$ACE2^+$ cells (Fig. 2A and B, respectively).

Despite the apparent lack of CPE in HCoV-NL63-infected 293T_$ACE2^+$ cells up to 7 days p.i., virus replication was examined by Western blotting with antibodies specific for the NL63-N protein. The results showed that viral protein was detectable in 293T_$ACE2^+$ and A549_$ACE2^+$ cells, suggesting that expression of the ACE2 protein rendered these cell lines permissive to infection by HCoV-NL63. No NL63-N protein was detected in WT cell lines (Fig. 3).

Coronaviruses employ a discontinuous replication strategy to generate sgmRNAs during minus-strand synthesis; these mRNAs are then copied into plus-strand mRNAs. Plus-stranded sgmRNA molecules are formed exclusively during virus replication and may therefore serve as markers for an active infection. Thus, we next examined WT and $ACE2^+$ cells for the presence of each HCoV-NL63 sgmRNA after virus inoculation. As shown in Fig. 4A, HCoV-NL63 sgmRNAs were formed in A549 and 293T cell lines expressing the ACE2 protein. Five mRNAs encoding viral structural and accessory proteins (spike [S], ORF3 protein, envelope [E], membrane [M], and nucleocapsid [N]) and genomic RNA were present, indicating active virus replication. No replication was noted in WT cells. These results confirm that ACE2 may act as a functional receptor for HCoV-NL63 virus.

Last but not least, viral replication kinetics was assessed by real-time PCR in cell lines supporting HCoV-NL63 replication

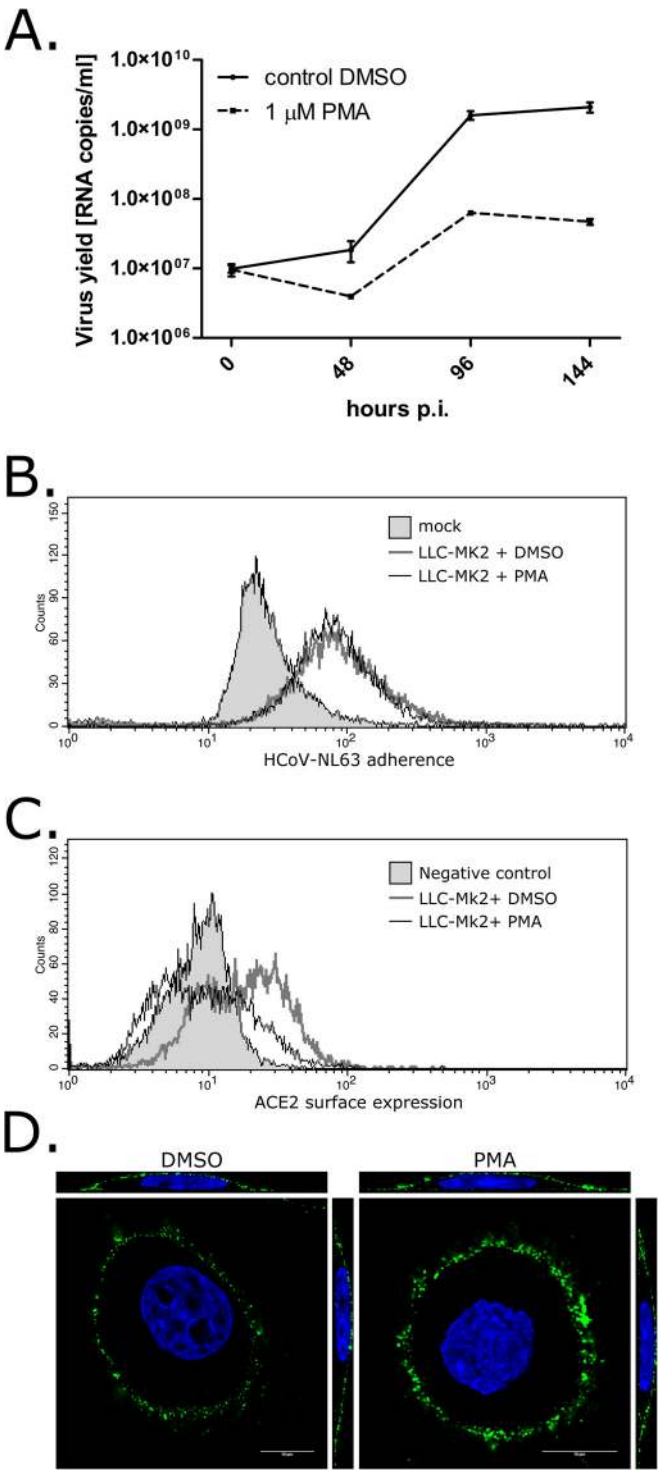

FIG 6 Adherence of HCoV-NL63 to LLC-Mk2 cells depleted of the ACE2 protein. LLC-Mk2 cells were depleted of surface ACE2 protein by incubation with 1 μM PMA and subsequently incubated with purified HCoV-NL63 or mock incubated. DMSO-treated cells were used as a control. (A) HCoV-NL63 replication on LLC-Mk2 ACE2$^+$ and ACE2$^-$ cells was evaluated with real-time PCR. A significant decrease in viral replication was observed on LLC-Mk2 cells pretreated with PMA compared to control cells. Data on virus replication are presented as the number of HCoV-NL63 RNA copies/ml. (B) Analysis of HCoV-NL63 adherence to ACE2$^+$ (+ DMSO) and ACE2$^-$ (+ PMA) LLC-Mk2 cells. HCoV-NL63 was labeled with specific antibodies, and virus adhesion was analyzed by flow cytometry. (C) A decrease in surface expression of the ACE2 protein on LLC-Mk2 cells after PMA treatment was confirmed using flow cytometry. (D) HCoV-NL63 adhesion to ACE2$^+$ (DMSO-treated) and ACE2$^-$ (PMA-treated) LLC-Mk2 cells was confirmed by confocal microscopy. LLC-Mk2 cells were pretreated with PMA or DMSO and incubated with purified HCoV-NL63. HCoV-NL63 virions are presented in green, while the blue denotes DNA. Each image is a single confocal plane (*xy*) with two orthogonal views (*xz* and *yz*) created by maximum projection of axial planes (thickness, 0.7 μm). Scale bar, 10 μm. The results shown are representative of at least three independent experiments.

(Fig. 4B). The results confirmed virus replication and progeny production in A549_ACE2$^+$ cells; a steep rise in the number of viral copies in the culture medium was observed already on day 3 p.i., corresponding in time with the first signs of CPE. No CPE or significant increase in viral yield was observed in 293T_WT/ACE2$^+$ cells.

Adhesion of HCoV-NL63 to mammalian cells. Next, a set of experiments to determine whether ACE2 serves as an attachment factor for HCoV-NL63 was performed. To address this, A549_WT and A549_ACE$^+$ cells were incubated at 4°C with gradient-purified HCoV-NL63, and virus adhesion to the cell surface was examined using flow cytometry. The virus bound to both cell lines, suggesting that a cell surface molecule other than ACE2 must be responsible for adhesion (Fig. 5).

Similarly, naturally permissive, normal (untreated) and PMA-treated (31) LLC-Mk2 cells were incubated at 4°C with gradient-purified HCoV-NL63, and virus adhesion to the cell surface was examined by flow cytometry. Even though PMA-mediated ACE2 scission inhibited replication of HCoV-NL63 (Fig. 6A), we observed no difference in virus attachment to normal and PMA-treated cells (Fig. 6B). Likewise, a decrease in cell surface ACE2 protein levels on LLC-Mk2 cells after PMA treatment was confirmed by flow cytometry (Fig. 6C).

To confirm the flow cytometry results, we used confocal microscopy to examine HCoV-NL63 adhesion to PMA-stimulated and normal LLC-Mk2 cells. A representative image is presented in Fig. 6D, which confirms that ACE2 shedding does not affect HCoV-NL63 binding to the cell surface.

Sialic acid or sugar moieties do not function as attachment receptors for HCoV-NL63. The results outlined above suggest that another molecule on the cell surface is responsible for virion attachment. Therefore, the role of sialic acid in virus adhesion was examined. To this end, HCoV-NL63 replication was analyzed in cells preincubated with *C. perfringens* type V neuraminidase, which shows a broad specificity for sialic acid-containing substrates (32). Flow cytometric analysis of HCoV-NL63 adhesion to LLC-Mk2 cells preincubated with neuraminidase showed no difference between control cells and cells lacking sialic acids and ACE2 (Fig. 7A to C). To ensure that sialic acid was enzymatically removed, influenza virus was used as a positive control. As expected, a significant inhibition of virus replication on A549 cells was observed after neuraminidase treatment as this common carbohydrate moiety represents a functional receptor for influenza viruses (data not shown).

Comparable experiments were undertaken to analyze whether lectins are responsible for HCoV-NL63 attachment to target cells. For this, several sugar monomers, such as D-(+)-galactose, D-(+)-mannose, D-(+)-*N*-acetylglucosamine, and L-(−)-fucose (33–35), were used in virus adhesion experiments on LLC-Mk2 cells. Additionally, D-(+)-glucose, a carbohydrate monomer,

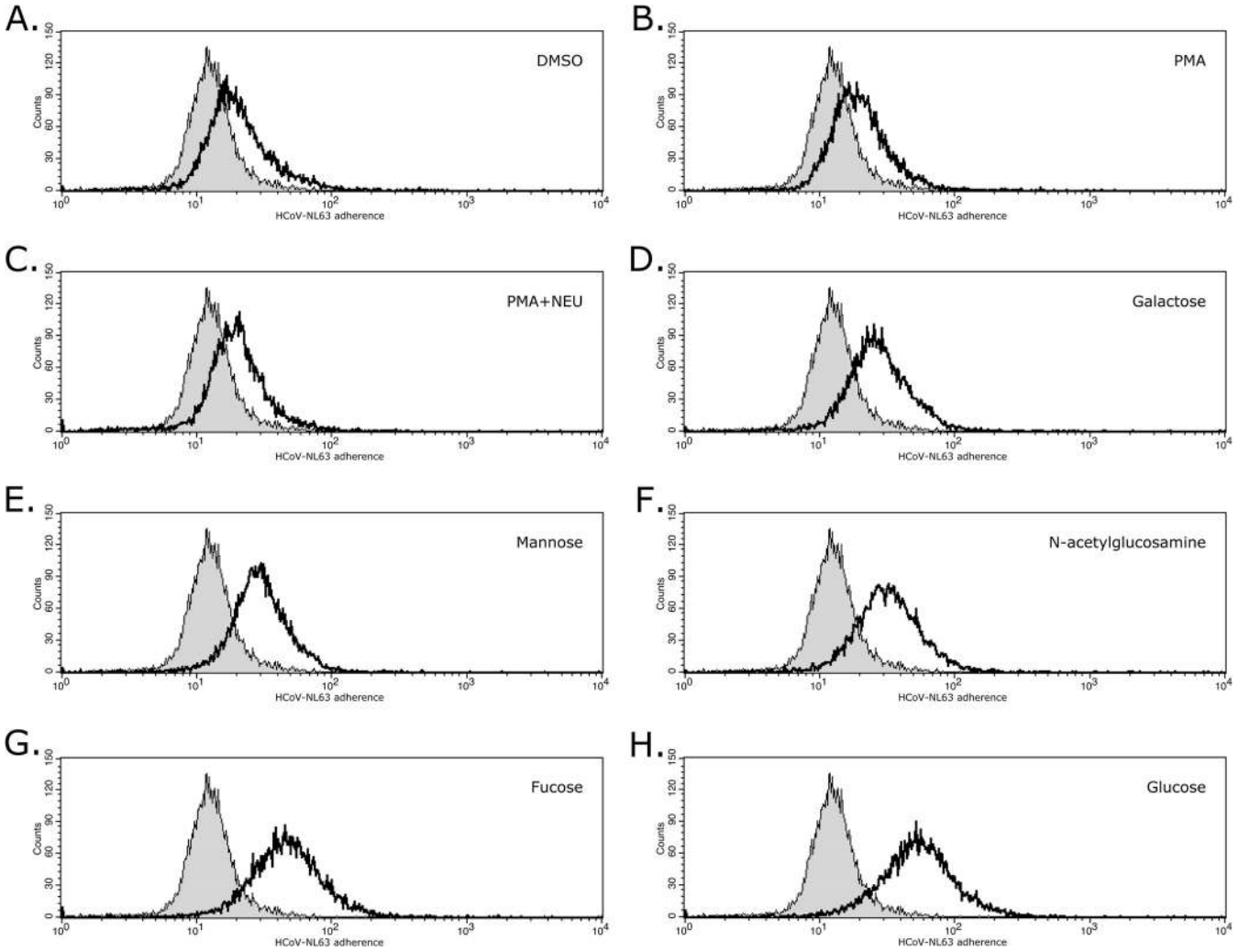

FIG 7 HCoV-NL63 adhesion to neuraminidase-treated cells and in the presence of sugar moieties. LLC-Mk2 cells were treated with DMSO (A), 1 μM PMA (B), or 1 μM PMA and 200 mU/ml type V neuraminidase (Neu) (C) and further incubated with purified HCoV-NL63 or mock incubated. Virus adhesion was assessed also in the presence of 50 mM sugar monomers: galactose (D), mannose (E), *N*-acetylglucosamine (F), fucose (G), or glucose (H), as a negative control. Virus adhesion was analyzed by flow cytometry. The results shown are representative of at least three independent experiments.

which does not constitute a ligand for known mammalian lectins, was included as a negative control. HCoV-NL63 adhesion to LLC-Mk2 in the presence of selected sugar moieties was analyzed using flow cytometry. No modulation of virus adhesion to the cell surface was observed (Fig. 7D to H).

Heparan sulfate inhibits virus attachment and entry. As HS proteoglycans are important for entry of several pathogens (36–50), a soluble HS was used to assess whether attachment of HCoV-NL63 is mediated by these molecules. Flow cytometric analysis demonstrated that in the presence of HS, virus adhesion to LLC-Mk2 cells was fully inhibited, showing the role of this molecule in adhesion to susceptible cells and possibly also in cell entry (Fig. 8A).

In order to analyze whether ACE2 protein participates in the virus attachment process, additional experiments were performed. For this, virus adhesion was analyzed in the presence of HS (to avoid the masking effect) on LLC-Mk2 cells with surface expression of ACE2 (dimethyl sulfoxide [DMSO]-treated) and on ACE2-depleted ($ACE2^-$; (PMA-treated) cells. Inhibition of virus-HS proteoglycan interaction resulted in lack of virus binding also on $ACE2^+$ cells; no difference between $ACE2^+$ and $ACE2^-$ cells was noted (Fig. 8A). Flow cytometry results were further confirmed by confocal microscopy (Fig. 8B).

Subsequent analysis showed that preincubation of the virus with HS results in a dose-dependent decline in virus replication (Fig. 9). Taken together, obtained results show that HS proteoglycans act as HCoV-NL63 adhesion receptors and that their presence is important for virus entry and replication.

DISCUSSION

Human coronavirus NL63 was first identified ~10 years ago. Since then, a number of research groups have studied this pathogen, resulting in the publication of a considerable number of papers about the virus's epidemiology and biology. Although at first glance HCoV-NL63 may simply be considered a close relative of HCoV-229E, the virus possesses several unique characteristics. The most striking is that it is the only alphacoronavirus to use the ACE2 protein for cellular entry (similarly to SARS-CoV). Because

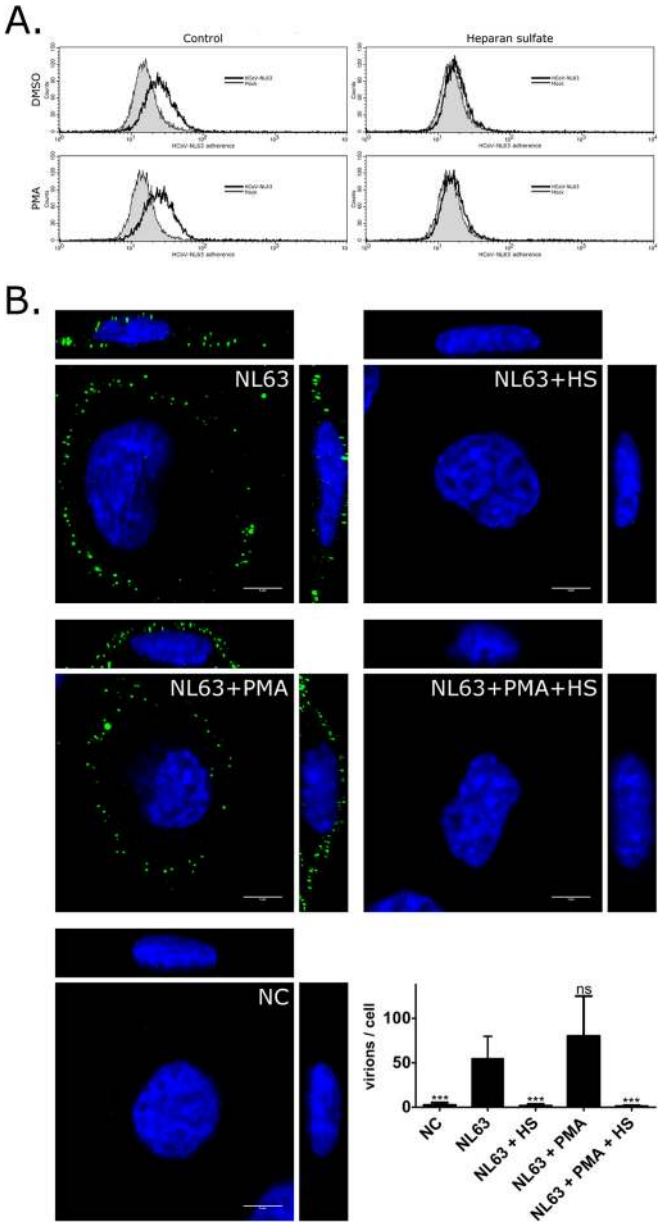

FIG 8 HCoV-NL63 adhesion to ACE2$^+$/ACE2$^-$ cells in the presence of heparan sulfate. (A) Flow cytometry analysis of HCoV-NL63 adhesion. The ACE2 protein was removed from the surface of LLC-Mk2 cells by incubation with 1 μM PMA (ACE2$^-$), while control cells were treated with DMSO (ACE2$^+$). Adhesion of HCoV-NL63 was assessed on ACE2$^+$ and ACE2$^-$ cells in the presence of 300 μg/ml HS or control PBS. (B) Confocal microscopy analysis of HCoV-NL63 adhesion. LLC-Mk2 cells were stimulated with 1 μM PMA or DMSO and incubated with purified HCoV-NL63 (NL63) in the presence or absence of heparan sulfate (HS). NC, cells incubated with the mock sample. HCoV-NL63 virions are presented in green, while the blue denotes DNA. Each image is a single confocal plane (*xy*) with two orthogonal views (*xz* and *yz*) created by maximum projection of axial planes (thickness, 4.8 μm). Scale bar, 5 μm. Bars in the graph represent the mean numbers of virions from 10 cells per sample ± standard errors.

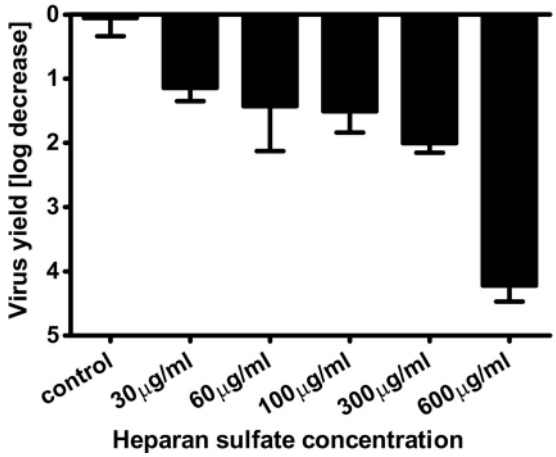

FIG 9 HCoV-NL63 replication in the presence of heparan sulfate. LLC-Mk2 cells were infected with HCoV-NL63 in the presence of increasing concentrations of HS or PBS. Virus replication in cell culture supernatants was evaluated using real-time PCR on day 4 p.i. Data on virus replication are presented as the number of HCoV-NL63 RNA copies/ml. All assays were performed in triplicate, and average values with standard errors (error bars) are presented. For all concentrations, the decrease in virus yield is statistically significant (Student's *t* test; $P < 0.05$).

these two pathogens use the same receptor, some investigators wonder why SARS-CoV infection manifests as life-threatening acute respiratory syndrome, while HCoV-NL63 infection results in a common cold. One hypothesis presented by Glowacka et al. assumes that HCoV-NL63-S shows only low affinity for the ACE2 protein; therefore, its infection efficiency is suboptimal (20). However, Wu et al. showed that the affinity of NL63-S for ACE2 is comparable with that of SARS-S (51). This discrepancy may result from the fact that Glowacka et al. used the complete S1 domain of HCoV-NL63-S, while Wu et al. used only the receptor-binding domain (RBD). Furthermore, in contrast to HCoV-NL63 infection, SARS-CoV infection results in a marked downregulation of ACE2 expression on the cell surface, thereby disrupting RAS homeostasis; this in itself may cause severe lung injury (20). Dijkman et al. showed that ACE2 expression was downregulated upon HCoV-NL63 infection although the result was heavily dependent upon the infection efficiency (52). Based on these reports, one wonders whether ACE2 is actually the cellular receptor for HCoV-NL63. The surface plasmon studies previously published by Glowacka et al. and Wu et al. suggest that NL63-S-RBD may interact with ACE2; however, another stimulus may be required to expose the RBD and enable its interaction with ACE2. That would suggest a similar strategy as one employed by HIV-1, where CD4 binding by gp120 results in structural alteration of the viral protein, which enables gp120 binding to coreceptors and subsequent entry (53).

Here, we showed that directed expression of ACE2 on cells previously resistant to HCoV-NL63 infection renders them susceptible. Next, we examined whether viral adherence was dependent upon the level of ACE2 expression. Comparative analyses using gradient-purified virus, WT cells, and cells overexpressing ACE2 showed that although ACE2 protein is a prerequisite for virus infection, it does not affect binding of virions to the cell surface. Also, selective scission of the ACE2 protein from the cell surface does not affect the virus-cell interaction.

These observations are consistent with reports showing that NL63-S protein has low affinity for ACE2 and suggest that another molecule/set of molecules may serve as attachment factors. In some betacoronaviruses, sialic acid may function as such a factor; however, we found that removing these surface molecules with

neuraminidase had no effect on HCoV-NL63 replication or attachment. Similarly, soluble sugars that should hinder the interaction between the potential lectin-like domain and cellular glycoproteins did not affect virus binding (33–35).

It has been reported that some beta- and gammacoronaviruses (SARS-CoV, culture adapted mouse hepatitis virus [MHV], and infectious bronchitis virus [IBV]) employ HS proteoglycans for adhesion or entry to susceptible cells (48–50). Therefore, the adhesion of the virus was evaluated in the presence of HS, a soluble receptor analog. Apparently, this compound blocked the ability of HCoV-NL63 to bind to the cell surface of susceptible cells, showing that HS proteoglycans are responsible for virus binding on cells. What is more, the presence of HS proteoglycans strongly enhances virus infection, showing the relevance of the observed phenomena.

One may, however, question whether the ability of HS binding was not acquired due to cell culture adaptation, as described for other coronaviral species (49, 54, 55). Analysis of the S gene shows that despite *in vitro* propagation of the Amsterdam I strain, no new potential HS binding sites can be identified compared to those of clinical isolates (data not shown). It is possible, however, that different HCoV-NL63 strains bind the HS with different affinities, which would explain the difficulty in acquiring new clinical isolates and the late identification of the pathogen (56, 57).

In summary, we examined whether human ACE2 (the receptor for HCoV-NL63) also serves as an attachment factor. HCoV-NL63 adhered equally well to ACE2-expressing and -nonexpressing cells. These observations indicated the existence of an additional molecule involved in HCoV-NL63 attachment to target cells. Competition experiments using a range of soluble elements of cellular membrane-associated components revealed that HS proteoglycans constitute HCoV-NL63 adhesion receptors. Importantly, the interaction of the virus with HS proteoglycans is important not only for virus binding but also for virus replication.

ACKNOWLEDGMENTS

This work was supported by an LIDER grant from the National Centre for Research and Development (Lider/27/55/L-2/10/2011), a grant from the Ministry of Science and Higher Education, Poland (Iuventus Plus grant IP2011 044371), and grants from the National Science Center (UMO-2012/07/E/NZ6/01712 and UMO-2012/07/N/NZ6/02955). The Faculty of Biochemistry, Biophysics and Biotechnology at Jagiellonian University is a beneficiary of structural funds from the European Union (grant no. POIG.02.01.00-12-064/08, Molecular Biotechnology for Health).

REFERENCES

1. **Knipe DM, Howley PM, Cohen JI, Griffin DE, Lamb RA, Martin MA, Rancaniello VR, Roizman B (ed)** 2013. Fields virology, 6th ed. Lippincott Williams & Wilkins, Philadelphia, PA.
2. **Peiris JS, Yuen KY, Osterhaus AD, Stohr K.** 2003. The severe acute respiratory syndrome. N. Engl. J. Med. **349:**2431–2441. http://dx.doi.org/10.1056/NEJMra032498.
3. **Stadler K, Masignani V, Eickmann M, Becker S, Abrignani S, Klenk HD, Rappuoli R.** 2003. SARS—beginning to understand a new virus. Nat. Rev. Microbiol. **1:**209–218. http://dx.doi.org/10.1038/nrmicro775.
4. **de Groot RJ, Baker SC, Baric RS, Brown CS, Drosten C, Enjuanes L, Fouchier RA, Galiano M, Gorbalenya AE, Memish ZA, Perlman S, Poon LL, Snijder EJ, Stephens GM, Woo PC, Zaki AM, Zambon M, Ziebuhr J.** 2013. Middle East respiratory syndrome coronavirus (MERS-CoV): announcement of the Coronavirus Study Group. J. Virol. **87:**7790–7792. http://dx.doi.org/10.1128/JVI.01244-13.
5. **Fouchier RA, Hartwig NG, Bestebroer TM, Niemeyer B, de Jong JC, Simon JH, Osterhaus AD.** 2004. A previously undescribed coronavirus associated with respiratory disease in humans. Proc. Natl. Acad. Sci. U. S. A. **101:**6212–6216. http://dx.doi.org/10.1073/pnas.0400762101.
6. **van der Hoek L, Pyrc K, Jebbink MF, Vermeulen-Oost W, Berkhout RJ, Wolthers KC, Wertheim-van Dillen PM, Kaandorp J, Spaargaren J, Berkhout B.** 2004. Identification of a new human coronavirus. Nat. Med. **10:**368–373. http://dx.doi.org/10.1038/nm1024.
7. **Pyrc K, Berkhout B, van der Hoek L.** 2007. The novel human coronaviruses NL63 and HKU1. J. Virol. **81:**3051–3057. http://dx.doi.org/10.1128/JVI.01466-06.
8. **van der Hoek L, Sure K, Ihorst G, Stang A, Pyrc K, Jebbink MF, Petersen G, Forster J, Berkhout B, Uberla K.** 2006. Human coronavirus NL63 infection is associated with croup. Advances in experimental medicine and biology. **581:**485–491. http://dx.doi.org/10.1007/978-0-387-33012-9_86.
9. **van der Hoek L, Sure K, Ihorst G, Stang A, Pyrc K, Jebbink MF, Petersen G, Forster J, Berkhout B, Uberla K.** 2005. Croup is associated with the novel coronavirus NL63. PLoS Med. **2:**e240. http://dx.doi.org/10.1371/journal.pmed.0020240.
10. **Pyrc K, Jebbink MF, Berkhout B, van der Hoek L.** 2004. Genome structure and transcriptional regulation of human coronavirus NL63. Virol. J. **1:**7. http://dx.doi.org/10.1186/1743-422X-1-7.
11. **Pyrc K, Dijkman R, Deng L, Jebbink MF, Ross HA, Berkhout B, van der Hoek L.** 2006. Mosaic structure of human coronavirus NL63, one thousand years of evolution. J. Mol. Biol. **364:**964–973. http://dx.doi.org/10.1016/j.jmb.2006.09.074.
12. **Gallagher TM, Buchmeier MJ.** 2001. Coronavirus spike proteins in viral entry and pathogenesis. Virology **279:**371–374. http://dx.doi.org/10.1006/viro.2000.0757.
13. **Zheng Q, Deng Y, Liu J, van der Hoek L, Berkhout B, Lu M.** 2006. Core structure of S2 from the human coronavirus NL63 spike glycoprotein. Biochemistry **45:**15205–15215. http://dx.doi.org/10.1021/bi061686w.
14. **Hofmann H, Pyrc K, van der Hoek L, Geier M, Berkhout B, Pohlmann S.** 2005. Human coronavirus NL63 employs the severe acute respiratory syndrome coronavirus receptor for cellular entry. Proc. Natl. Acad. Sci. U. S. A. **102:**7988–7993. http://dx.doi.org/10.1073/pnas.0409465102.
15. **Hofmann H, Marzi A, Gramberg T, Geier M, Pyrc K, van der Hoek L, Berkhout B, Pohlmann S.** 2006. Attachment factor and receptor engagement of SARS coronavirus and human coronavirus NL63. Adv. Exp. Med. Biol. **581:**219–227. http://dx.doi.org/10.1007/978-0-387-33012-9_37.
16. **Pohlmann S, Gramberg T, Wegele A, Pyrc K, van der Hoek L, Berkhout B, Hofmann H.** 2006. Interaction between the spike protein of human coronavirus NL63 and its cellular receptor ACE2. Adv. Exp. Med. Biol. **581:**281–284. http://dx.doi.org/10.1007/978-0-387-33012-9_47.
17. **Donoghue M, Hsieh F, Baronas E, Godbout K, Gosselin M, Stagliano N, Donovan M, Woolf B, Robison K, Jeyaseelan R, Breitbart RE, Acton S.** 2000. A novel angiotensin-converting enzyme-related carboxypeptidase (ACE2) converts angiotensin I to angiotensin 1-9. Circ. Res. **87:**E1–E9. http://dx.doi.org/10.1161/01.RES.87.5.e1.
18. **Rice GI, Thomas DA, Grant PJ, Turner AJ, Hooper NM.** 2004. Evaluation of angiotensin-converting enzyme (ACE), its homologue ACE2 and neprilysin in angiotensin peptide metabolism. Biochem. J. **383:**45–51. http://dx.doi.org/10.1042/BJ20040634.
19. **Tipnis SR, Hooper NM, Hyde R, Karran E, Christie G, Turner AJ.** 2000. A human homolog of angiotensin-converting enzyme. Cloning and functional expression as a captopril-insensitive carboxypeptidase. J. Biol. Chem. **275:**33238–33243. http://dx.doi.org/10.1074/jbc.M002615200.
20. **Glowacka I, Bertram S, Herzog P, Pfefferle S, Steffen I, Muench MO, Simmons G, Hofmann H, Kuri T, Weber F, Eichler J, Drosten C, Pohlmann S.** 2010. Differential downregulation of ACE2 by the spike proteins of severe acute respiratory syndrome coronavirus and human coronavirus NL63. J. Virol. **84:**1198–1205. http://dx.doi.org/10.1128/JVI.01248-09.
21. **Kuba K, Imai Y, Rao S, Gao H, Guo F, Guan B, Huan Y, Yang P, Zhang Y, Deng W, Bao L, Zhang B, Liu G, Wang Z, Chappell M, Liu Y, Zheng D, Leibbrandt A, Wada T, Slutsky AS, Liu D, Qin C, Jiang C, Penninger JM.** 2005. A crucial role of angiotensin converting enzyme 2 (ACE2) in SARS coronavirus-induced lung injury. Nat. Med. **11:**875–879. http://dx.doi.org/10.1038/nm1267.
22. **Li W, Moore MJ, Vasilieva N, Sui J, Wong SK, Berne MA, Somasundaran M, Sullivan JL, Luzuriaga K, Greenough TC, Choe H, Farzan M.** 2003. Angiotensin-converting enzyme 2 is a functional receptor for the SARS coronavirus. Nature **426:**450–454. http://dx.doi.org/10.1038/nature02145.

23. **Li W, Sui J, Huang IC, Kuhn JH, Radoshitzky SR, Marasco WA, Choe H, Farzan M.** 2007. The S proteins of human coronavirus NL63 and severe acute respiratory syndrome coronavirus bind overlapping regions of ACE2. Virology **367:**367–374. http://dx.doi.org/10.1016/j.virol.2007.04.035.
24. **Hattermann K, Muller MA, Nitsche A, Wendt S, Donoso Mantke O, Niedrig M.** 2005. Susceptibility of different eukaryotic cell lines to SARS-coronavirus. Arch. Virol. **150:**1023–1031. http://dx.doi.org/10.1007/s00705-004-0461-1.
25. **Hofmann H, Hattermann K, Marzi A, Gramberg T, Geier M, Krumbiegel M, Kuate S, Uberla K, Niedrig M, Pohlmann S.** 2004. S protein of severe acute respiratory syndrome-associated coronavirus mediates entry into hepatoma cell lines and is targeted by neutralizing antibodies in infected patients. J. Virol. **78:**6134–6142. http://dx.doi.org/10.1128/JVI.78.12.6134-6142.2004.
26. **Schildgen O, Jebbink MF, de Vries M, Pyrc K, Dijkman R, Simon A, Muller A, Kupfer B, van der Hoek L.** 2006. Identification of cell lines permissive for human coronavirus NL63. J. Virol. Methods **138:**207–210. http://dx.doi.org/10.1016/j.jviromet.2006.07.023.
27. **Mathewson AC, Bishop A, Yao Y, Kemp F, Ren J, Chen H, Xu X, Berkhout B, van der Hoek L, Jones IM.** 2008. Interaction of severe acute respiratory syndrome-coronavirus and NL63 coronavirus spike proteins with angiotensin converting enzyme-2. J. Gen. Virol. **89:**2741–2745. http://dx.doi.org/10.1099/vir.0.2008/003962-0.
28. **Moffat J, Grueneberg DA, Yang X, Kim SY, Kloepfer AM, Hinkle G, Piqani B, Eisenhaure TM, Luo B, Grenier JK, Carpenter AE, Foo SY, Stewart SA, Stockwell BR, Hacohen N, Hahn WC, Lander ES, Sabatini DM, Root DE.** 2006. A lentiviral RNAi library for human and mouse genes applied to an arrayed viral high-content screen. Cell **124:**1283–1298. http://dx.doi.org/10.1016/j.cell.2006.01.040.
29. **Reed LJ, Muench H.** 1938. A simple method of estimating fifty per cent endpoints. Am. J. Epidemiol. **27:**493–497.
30. **Bolte S, Cordelieres FP.** 2006. A guided tour into subcellular colocalization analysis in light microscopy. J. Microsc. **224:**213–232. http://dx.doi.org/10.1111/j.1365-2818.2006.01706.x.
31. **Lai ZW, Hanchapola I, Steer DL, Smith AI.** 2011. Angiotensin-converting enzyme 2 ectodomain shedding cleavage-site identification: determinants and constraints. Biochemistry **50:**5182–5194. http://dx.doi.org/10.1021/bi200525y.
32. **Rauvala H.** 1979. Monomer-micelle transition of the ganglioside GM1 and the hydrolysis by *Clostridium perfringens* neuraminidase. Eur. J. Biochem. **97:**555–564. http://dx.doi.org/10.1111/j.1432-1033.1979.tb13144.x.
33. **Klimstra WB, Nangle EM, Smith MS, Yurochko AD, Ryman KD.** 2003. DC-SIGN and L-SIGN can act as attachment receptors for alphaviruses and distinguish between mosquito cell- and mammalian cell-derived viruses. J. Virol. **77:**12022–12032. http://dx.doi.org/10.1128/JVI.77.22.12022-12032.2003.
34. **Alvarez CP, Lasala F, Carrillo J, Muniz O, Corbi AL, Delgado R.** 2002. C-type lectins DC-SIGN and L-SIGN mediate cellular entry by Ebola virus in *cis* and in *trans*. J. Virol. **76:**6841–6844. http://dx.doi.org/10.1128/JVI.76.13.6841-6844.2002.
35. **Zhang Y, Buckles E, Whittaker GR.** 2012. Expression of the C-type lectins DC-SIGN or L-SIGN alters host cell susceptibility for the avian coronavirus, infectious bronchitis virus. Vet. Microbiol. **157:**285–293. http://dx.doi.org/10.1016/j.vetmic.2012.01.011.
36. **Sureau C, Salisse J.** 2013. A conformational heparan sulfate binding site essential to infectivity overlaps with the conserved hepatitis B virus a-determinant. Hepatology **57:**985–994. http://dx.doi.org/10.1002/hep.26125.
37. **Lamas Longarela O, Schmidt TT, Schoneweis K, Romeo R, Wedemeyer H, Urban S, Schulze A.** 2013. Proteoglycans act as cellular hepatitis delta virus attachment receptors. PLoS One **8:**e58340. http://dx.doi.org/10.1371/journal.pone.0058340.
38. **Kobayashi K, Kato K, Sugi T, Takemae H, Pandey K, Gong H, Tohya Y, Akashi H.** 2010. *Plasmodium falciparum* BAEBL binds to heparan sulfate proteoglycans on the human erythrocyte surface. J. Biol. Chem. **285:**1716–1725. http://dx.doi.org/10.1074/jbc.M109.021576.
39. **Bucior I, Pielage JF, Engel JN.** 2012. Pseudomonas aeruginosa pili and flagella mediate distinct binding and signaling events at the apical and basolateral surface of airway epithelium. PLoS Pathog. **8:**e1002616. http://dx.doi.org/10.1371/journal.ppat.1002616.
40. **Norman MU, Moriarty TJ, Dresser AR, Millen B, Kubes P, Chaconas G.** 2008. Molecular mechanisms involved in vascular interactions of the Lyme disease pathogen in a living host. PLoS Pathog. **4:**e1000169. http://dx.doi.org/10.1371/journal.ppat.1000169.
41. **Lebrun P, Raze D, Fritzinger B, Wieruszeski JM, Biet F, Dose A, Carpentier M, Schwarzer D, Allain F, Lippens G, Locht C.** 2012. Differential contribution of the repeats to heparin binding of HBHA, a major adhesin of *Mycobacterium tuberculosis*. PLoS One **7:**e32421. http://dx.doi.org/10.1371/journal.pone.0032421.
42. **Germi R, Crance JM, Garin D, Guimet J, Lortat-Jacob H, Ruigrok RW, Zarski JP, Drouet E.** 2002. Cellular glycosaminoglycans and low density lipoprotein receptor are involved in hepatitis C virus adsorption. J. Med. Virol. **68:**206–215. http://dx.doi.org/10.1002/jmv.10196.
43. **Kalia M, Chandra V, Rahman SA, Sehgal D, Jameel S.** 2009. Heparan sulfate proteoglycans are required for cellular binding of the hepatitis E virus ORF2 capsid protein and for viral infection. J. Virol. **83:**12714–12724. http://dx.doi.org/10.1128/JVI.00717-09.
44. **Cruz L, Meyers C.** 2013. Differential dependence on host cell glycosaminoglycans for infection of epithelial cells by high-risk HPV types. PLoS One **8:**e68379. http://dx.doi.org/10.1371/journal.pone.0068379.
45. **Shukla D, Liu J, Blaiklock P, Shworak NW, Bai X, Esko JD, Cohen GH, Eisenberg RJ, Rosenberg RD, Spear PG.** 1999. A novel role for 3-O-sulfated heparan sulfate in herpes simplex virus 1 entry. Cell **99:**13–22. http://dx.doi.org/10.1016/S0092-8674(00)80058-6.
46. **Lambert S, Bouttier M, Vassy R, Seigneuret M, Petrow-Sadowski C, Janvier S, Heveker N, Ruscetti FW, Perret G, Jones KS, Pique C.** 2009. HTLV-1 uses HSPG and neuropilin-1 for entry by molecular mimicry of VEGF165. Blood **113:**5176–5185. http://dx.doi.org/10.1182/blood-2008-04-150342.
47. **Patel M, Yanagishita M, Roderiquez G, Bou-Habib DC, Oravecz T, Hascall VC, Norcross MA.** 1993. Cell-surface heparan sulfate proteoglycan mediates HIV-1 infection of T-cell lines. AIDS Res. Hum. Retroviruses **9:**167–174. http://dx.doi.org/10.1089/aid.1993.9.167.
48. **Watanabe R, Sawicki SG, Taguchi F.** 2007. Heparan sulfate is a binding molecule but not a receptor for CEACAM1-independent infection of murine coronavirus. Virology **366:**16–22. http://dx.doi.org/10.1016/j.virol.2007.06.034.
49. **Madu IG, Chu VC, Lee H, Regan AD, Bauman BE, Whittaker GR.** 2007. Heparan sulfate is a selective attachment factor for the avian coronavirus infectious bronchitis virus Beaudette. Avian Dis. **51:**45–51. http://dx.doi.org/10.1637/0005-2086(2007)051[0045:HSIASA]2.0.CO;2.
50. **Lang J, Yang N, Deng J, Liu K, Yang P, Zhang G, Jiang C.** 2011. Inhibition of SARS pseudovirus cell entry by lactoferrin binding to heparan sulfate proteoglycans. PLoS One **6:**e23710. http://dx.doi.org/10.1371/journal.pone.0023710.
51. **Wu K, Chen L, Peng G, Zhou W, Pennell CA, Mansky LM, Geraghty RJ, Li F.** 2011. A virus-binding hot spot on human angiotensin-converting enzyme 2 is critical for binding of two different coronaviruses. J. Virol. **85:**5331–5337. http://dx.doi.org/10.1128/JVI.02274-10.
52. **Dijkman R, Jebbink MF, Deijs M, Milewska A, Pyrc K, Buelow E, van der Bijl A, van der Hoek L.** 2012. Replication-dependent downregulation of cellular angiotensin-converting enzyme 2 protein expression by human coronavirus NL63. J. Gen. Virol. **93:**1924–1929. http://dx.doi.org/10.1099/vir.0.043919-0.
53. **Wilen CB, Tilton JC, Doms RW.** 2012. HIV: cell binding and entry. Cold Spring Harb. Perspect. Med. **2:**a006866. http://dx.doi.org/10.1101/cshperspect.a006866.
54. **de Haan CA, Haijema BJ, Schellen P, Wichgers Schreur P, te Lintelo E, Vennema H, Rottier PJ.** 2008. Cleavage of group 1 coronavirus spike proteins: how furin cleavage is traded off against heparan sulfate binding upon cell culture adaptation. J. Virol. **82:**6078–6083. http://dx.doi.org/10.1128/JVI.00074-08.
55. **de Haan CA, Li Z, te Lintelo E, Bosch BJ, Haijema BJ, Rottier PJ.** 2005. Murine coronavirus with an extended host range uses heparan sulfate as an entry receptor. J. Virol. **79:**14451–14456. http://dx.doi.org/10.1128/JVI.79.22.14451-14456.2005.
56. **Dijkman R, Jebbink MF, Koekkoek SM, Deijs M, Jonsdottir HR, Molenkamp R, Ieven M, Goossens H, Thiel V, van der Hoek L.** 2013. Isolation and characterization of current human coronavirus strains in primary human epithelial cell cultures reveal differences in target cell tropism. J. Virol. **87:**6081–6090. http://dx.doi.org/10.1128/JVI.03368-12.
57. **van der Hoek L, Pyrc K, Berkhout B.** 2006. Human coronavirus NL63, a new respiratory virus. FEMS Microbiol. Rev. **30:**760–773. http://dx.doi.org/10.1111/j.1574-6976.2006.00032.x.